Table 2.7.4.1. *Monolithic monochromator for plane-wave synchrotron-radiation topography*

| | |
|---|---|
| Reflection 1 | $\bar{3}33$ |
| Reflection 2 | $\bar{1}3\bar{1}$ |
| Reflection 3 | $1\bar{3}\bar{1}$ |
| Output wavelength | 0.12378 nm |
| Spectral pass band, $d\lambda/\lambda$ | $\sim 7 \times 10^{-6}$ |
| Angular divergence of exit beam | $\sim 1.4 \times 10^{-6}$ |
| Size of exit beam | $15 \times 15$ mm |

incident on the specimen crystal, the three crystals together forming a $+ + -$ arrangement (Ishikawa, Kitano & Matsui, 1985). The first monochromator is oriented for asymmetric $11\bar{1}$ Bragg reflection, the second for highly asymmetric $55\bar{3}$ reflection ($W_{out}/W_{in} = 64$ at $\lambda = 0.12$ nm), resulting in a divergence of only $0.5 \times 10^{-6}$ in the beam impinging on the specimen.

Multireflection systems, some of which were proposed by Du Mond (1937) but not at that time realizable, have become a practicality through the advent of perfect silicon and germanium. When multiple reflection occurs between the walls of a channel cut in a perfect crystal, the tails of the curve of angular dependence of reflection intensity can be greatly attenuated without much loss of reflectivity at the peak of the curve (Bonse & Hart, 1965*a*). Beaumont & Hart (1974) described combinations of such 'channel-cut' monochromators that were suitable for use with synchrotron sources. One combination, consisting of a pair of contra-rotating channel-cut crystals, with each channel acting as a pair of reflecting surfaces in symmetrical $+ -$ setting, has found much favour as a monochromatizing device producing neither angular deviation nor spatial displacement of the final beam, whatever the wavelength it is set to pass. The properties of monoliths with one or more channels and employing two or more asymmetric reflections in succession have been analysed by Kikuta & Kohra (1970), Kikuta (1971), and Matsushita, Kikuta & Kohra (1971).

Symmetric channel-cut monochromators in perfect undistorted crystals transmit harmonic reflections. Several approaches to the problem of harmonic elimination may be taken, such as one of the following procedures (or possibly more than one in combination).

(1) Using crystals of slightly different interplanar spacing (*e.g.* silicon and germanium) in the $+ -$ setting, which then becomes slightly dispersive (Bonse, Materlik & Schröder, 1976; Bauspiess, Bonse, Graeff & Rauch, 1977).

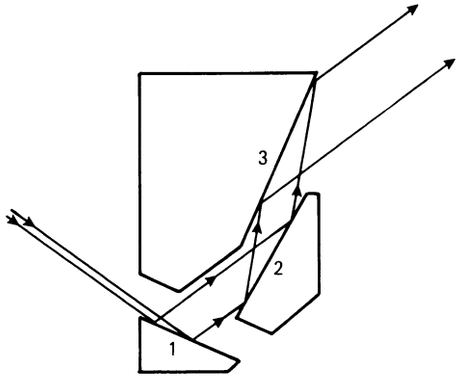


Fig. 2.7.4.1. Monolithic multiply reflecting monochromator for plane-wave topography.

(2) Laue case (transmission) followed by Bragg case (reflection), with deliberate slight misorientation between the diffracting elements (Materlik & Kostroun, 1980).

(3) Asymmetric reflection in non-parallel channel walls in a monolith (Hashizume, 1983).

(4) Misorientating a multiply reflecting channel, either one wall with respect to the opposite wall, or one length segment with respect to a following length segment (Hart & Rodrigues, 1978; Bonse, Olthoff-Münter & Rumpf, 1983; Hart, Rodrigues & Siddons, 1984).

For X-ray topographic applications, it is very desirable to have a spatially wide beam issuing from the multiply reflecting device. This is achieved, together with small angular divergence and spectral window, and without need of mechanical bending, in a monolith design by Hashizume, though it lacks wavelength tunability (Petroff, Sauvage, Riglet & Hashizume, 1980). The configuration of reflecting surfaces of this monolith is shown in Fig. 2.7.4.1. Reflection occurs in succession at surfaces 1, 2, and 3. The monochromator characteristics are listed in Table 2.7.4.1. The wavelength is very suitable in many topographic applications, and this design has proved to be an effective beam conditioner for use in synchrotron-radiation 'plane-wave' topography.

## 2.7.5. Some special techniques

### 2.7.5.1. *Moiré topography*

In X-ray optics, the same basic geometrical interpretation of moiré patterns applies as in light and electron optics. Suppose radiation passes successively through two periodic media, (1) and (2), whose reciprocal vectors are $\mathbf{h}_1$ and $\mathbf{h}_2$, so as to form a moiré pattern. Then, the reciprocal vector of the moiré fringes will be $\mathbf{H} = \mathbf{h}_1 - \mathbf{h}_2$. The magnitude, $D$, of the moiré fringe spacing is $|\mathbf{H}|^{-1}$ and may typically lie in the range 0.1 to 1 mm in the case of X-ray moiré patterns. Simple special cases are the 'rotation' moiré pattern in which $|\mathbf{h}_1| = |\mathbf{h}_2| = d^{-1}$, but $\mathbf{h}_1$ makes a small angle $\alpha$ with $\mathbf{h}_2$. Then, the spacing of the moiré fringes is $d/\alpha$ and the fringes run parallel to the bisector of the small angle $\alpha$. The other special case is the 'compression' moiré pattern. Here, $\mathbf{h}_1$ and $\mathbf{h}_2$ are parallel but there is a small difference between their corresponding spacings, $d_1$ and $d_2$. The spacing $D$ of compression moiré fringes is given by $D = d_1 d_2/(d_1 - d_2)$ and the fringes lie parallel to the grating rulings or Bragg planes in (1) and (2). X-ray moiré topographs achieve sensitivies of $10^{-7}$ to $10^{-8}$ in measuring orientation differences or relative differences in interplanar spacing. Moreover, if either periodic medium contains a lattice dislocation, Burgers vector $\mathbf{b}$, for which $\mathbf{b} \cdot \mathbf{h} \neq 0$, then a magnified image of the dislocation will appear in the moiré pattern, as one or more fringes terminating at the position of the dislocation, the number of terminating fringes being $\mathbf{b} \cdot \mathbf{h}$, which is necessarily integral (Hashimoto & Uyeda, 1957).

X-ray moiré topography has been performed with two quite different arrangements, the Bonse & Hart interferometer, and by superposition of separate crystals (Brádler & Lang, 1968). For accounts of the principles and applications of the interferometer, see, for example, Bonse & Hart (1965*b*, 1966), Hart (1968, 1975*b*), Bonse & Graeff (1977), Section 4.2.6 and §4.2.6.3.1. Fig. 2.7.5.1 shows the arrangement (Hart, 1968, 1972) for obtaining large-area moiré topographs by traversing the interferometer relative to a ribbon incident beam in similar fashion to taking a normal projection topograph (Fig. 2.7.2.2); $P$ is the incident-beam slit, $Q$ is a





references